

# Chapter 5

## The Witten-Veneziano formula

---

In this chapter we compute the decay constant of the  $\eta$  meson,  $F_\eta$ , in two dimensions and attempt to make a connection to the value of  $F_\pi$  that we measured in the previous chapter. To do so we rely on the Witten-Veneziano formula [1,2], which in 3-flavor QCD relates the mass of the  $\eta'$  meson with  $m_\eta$ ,  $m_K$ ,  $F_\pi$  and the quenched *topological susceptibility*  $\chi_T^{\text{que}}$ , defined below. This formula is obtained by taking the 't Hooft limit of a  $1/N_c$  expansion, where  $N_c$  is the number of colors. In this limit one considers  $N_c \rightarrow \infty$  and  $g_s \rightarrow 0$ , while leaving the product  $g^2 = g_s^2 N_c$  finite ( $g_s$  is the strong coupling constant).

In theory one introduces two  $\eta$  mesons, with the valence quark composition

$$\eta_1 = \frac{1}{\sqrt{3}} (\bar{u}u + \bar{d}d + \bar{s}s), \quad \eta_8 = \frac{1}{\sqrt{6}} (\bar{u}u + \bar{d}d - 2\bar{s}s). \quad (5.1)$$

$\eta_1$  is a flavor singlet and  $\eta_8$  belongs to an octet of states. In nature one observes the particles  $\eta$  and  $\eta'$ , which are mixed by an angle  $\theta_P$

$$\begin{pmatrix} \eta \\ \eta' \end{pmatrix} = \begin{pmatrix} \cos \theta_P & -\sin \theta_P \\ \sin \theta_P & \cos \theta_P \end{pmatrix} \begin{pmatrix} \eta_8 \\ \eta_1 \end{pmatrix}. \quad (5.2)$$

Since the measured value of  $\theta_P$  is small,  $\theta_P = -11.3^\circ$  [3], we have

$$\eta \approx \frac{1}{\sqrt{6}} (\bar{u}u + \bar{d}d - 2\bar{s}s), \quad \eta' \approx \frac{1}{\sqrt{3}} (\bar{u}u + \bar{d}d + \bar{s}s). \quad (5.3)$$

Veneziano [2] obtained the following formula by taking into account the three lightest quark flavors and assuming  $m_u = m_d = 0$  and  $m_s > 0$  to order  $1/N_c$

$$m_{\eta'}^2 + m_\eta^2 - 2m_K^2 = \frac{6}{F_{\eta'}^2} \chi_T^{\text{que}}. \quad (5.4)$$

where  $F_{\eta'}$  is the decay constant of the meson  $\eta'$  and “que” stands for quenched, *i.e.* its value when the degenerate fermion mass  $m \rightarrow \infty$ . In the chiral limit we obtain the formula deduced by Witten

$$m_{\eta'}^2 = \frac{6}{F_{\eta'}^2} \chi_T^{\text{que}}. \quad (5.5)$$

To lowest order in a  $1/N_c$  expansion, we have  $F_{\eta'} = F_\pi$  [1]. This leads to the question if this relation between the decay constants holds in the Schwinger model. In general, the literature refers to eq. (5.4) or (5.5), as the Witten-Veneziano formula.

In the two-flavor Schwinger model, in the limit of massless fermions, eq. (5.4) is simplified to<sup>1</sup> [4, 5]

$$m_\eta^2 = \frac{2N}{F_\eta^2} \chi_T^{\text{que}}, \quad (5.6)$$

where  $N$  is the number of flavors. We compute  $F_\eta$  in the Schwinger model with eq. (5.6) and based on the result we verify whether the relation  $F_\eta \simeq F_\pi$  holds. This would also enable us to determine  $F_\pi$  by an independent method that does not involve the  $\delta$ -regime.

The topological susceptibility  $\chi_T$  is defined for the Euclidean Schwinger model in the continuum as

$$\chi_T = \int d^2x (\langle q(x)q(0) \rangle - \langle q(x) \rangle \langle q(0) \rangle), \quad (5.7)$$

where

$$q(x) = \frac{g}{4\pi} \epsilon_{\mu\nu} F_{\mu\nu}(x) = \frac{g}{2\pi} F_{12}(x) \quad (5.8)$$

is the *topological charge density*. With  $q(x)$  we define the *topological charge* as

$$Q = \int d^2x q(x) \in \mathbb{Z}. \quad (5.9)$$

We can formulate  $\chi_T$  in terms of  $Q$  as well

$$\chi_T = \frac{\langle Q^2 \rangle - \langle Q \rangle^2}{V}, \quad (5.10)$$

where  $V$  is the space-time volume. An important property of the topological charge is that it is an integer number. We can see that fact if we rewrite  $q(x)$  as a total divergence

$$q(x) = \partial_\mu \Omega_\mu(x), \quad \Omega_\mu(x) = \frac{g}{2\pi} \epsilon_{\mu\nu} A_\nu(x). \quad (5.11)$$

If we consider field configurations of finite action,  $F_{\mu\nu}(x)$  has to vanish at infinity, so the gauge field must be gauge equivalent to 0 when  $|x| \rightarrow \infty$

$$0 = A'_\mu(x) = A_\mu(x) - \frac{1}{g} \partial_\mu \varphi(x). \quad (5.12)$$

Then

$$Q = \int d^2x \partial_\mu \left( \frac{g}{2\pi} \epsilon_{\mu\nu} \frac{1}{g} \partial_\nu \varphi(x) \right) = \frac{1}{2\pi} \int_{\partial V} d\sigma_\mu \epsilon_{\mu\nu} \partial_\nu \varphi(x), \quad (5.13)$$

where we have used the Gauss theorem and where we assume  $\partial V$  to be the boundary of a large volume in  $\mathbb{R}^2$ . Now, if we consider a circumference of length  $L$ , we identify  $Q$  with the following integral

$$\lim_{L \rightarrow \infty} \frac{1}{2\pi i} \int_0^L dx U^*(x) \partial_x U(x), \quad \text{where } U(x) = e^{i\varphi(x)}, \quad U(L) = U(0). \quad (5.14)$$

This expression is equal to

$$\frac{1}{2\pi} [\varphi(L) - \varphi(0)] = n \in \mathbb{Z}, \quad (5.15)$$

hence  $Q$  is an integer.

---

<sup>1</sup>One can make an analogy of the flavor singlet of the two-flavor Schwinger model,  $(\bar{u}u + \bar{d}d)/\sqrt{2}$ , with the singlet  $\eta_1$  of QCD. Since  $\eta_1$  is close to  $\eta'$ , in the literature they often refer to the flavor singlet of the two-flavor Schwinger model as  $\eta'$  [4, 5]. However, it is not the actual  $\eta'$  particle from QCD and for simplicity we will denote it as  $\eta$ .

As we mentioned in Chapter 3, we can relate  $m_\eta$  with the gauge coupling as follows

$$m_\eta^2 = N \frac{g^2}{\pi}. \quad (5.16)$$

Thus, by determining  $\chi_T^{\text{que}}$  we obtain a value for  $F_\eta$ . According to refs. [4,5], the theoretical expression for  $\chi_T^{\text{que}}$  in infinite volume and in the continuum is

$$\chi_T^{\text{que}} = \frac{g^2}{4\pi^2} \simeq 0.0253 g^2. \quad (5.17)$$

This implies that theoretically  $F_\eta = 0.3989$ . This result was also deduced in ref. [6].

To numerically measure the topological susceptibility by using lattice simulations we have to discretize the topological charge density. This can be done most easily through the plaquette variables defined in Chapter 2. From eq. (2.94), we know that for a small lattice spacing  $a$ , the plaquette variables have the following expression

$$U_{\mu\nu}(\vec{n}) = e^{iga^2 F_{\mu\nu}(\vec{n})}, \quad F_{\mu\nu}(\vec{n}) = -\frac{i}{ga^2} \ln U_{\mu\nu}(\vec{n}). \quad (5.18)$$

That way, we have

$$q(\vec{n}) = -\frac{i}{2\pi a^2} \ln U_{12}(\vec{n}) \quad (5.19)$$

and

$$Q = \sum_{\vec{n}} a^2 q(\vec{n}), \quad (5.20)$$

where the sum runs over all lattice sites  $\{\vec{n} = (n_1, n_2) | n_\mu = 0, 1, \dots, N_\mu - 1; \mu = 1, 2\}$ .

The lattice configurations generated through Monte Carlo algorithms are sorted in different sectors, where each one is characterized by a topological charge. Furthermore, there is evidence (see e.g. refs. [7,8]) that the distribution of these configurations corresponds approximately to a Gaussian function. Due to parity symmetry, we also have

$$\langle Q \rangle = 0. \quad (5.21)$$

Then, one can calculate  $\chi_T$  on the lattice using the following weighted average

$$\chi_T = \frac{\sum_Q Q^2 N_Q}{V \sum_Q N_Q}, \quad (5.22)$$

where  $N_Q$  are the number of configurations in the topological sector labeled by  $Q$ .

In Chapter 5 we have shown the histograms for  $Q$  obtained with simulations for several lattice sizes, using low statistics ( $10^3$  measurements separated by 10 sweeps). We attempted to compute the topological susceptibility using those results. Unfortunately, even though the topological charge is compatible with  $\langle Q \rangle = 0$ ,  $\chi_T$  as a function of the fermion mass  $m$  does not have a clear behavior, see for instance figure 5.1. This does not allow us to perform a fit and to extrapolate to the quenched value of  $\chi_T$ . Usually the autocorrelation time for  $Q$  is larger than with other observables. Separating the measurements by 10 sweeps could be enough to decorrelate other observables, but here we see that it affects the result of  $\chi_T$ . For that reason, we incremented the number of measurements to  $10^4$ , separated by 100 sweeps, and simulated a  $10 \times 64$  lattice for  $\beta = 4$ . This improved the results. In figure 5.2 we show the distribution of the configurations and in figure 5.3 we show the topological susceptibility as a function of the degenerate fermion mass. We used two functions to extrapolate  $\chi_T$ , from their average we obtain

$$\chi_T^{\text{que}} \beta = 0.029(1). \quad (5.23)$$

This result is in agreement with ref. [9], which reported  $\chi_T^{\text{que}}\beta = 0.0300(8)$  at  $\beta = 4$ , and with our quenched simulations  $\chi_T^{\text{que}}\beta = 0.0304(2)$  (see below).

Now, we substitute eq. (5.16) in eq. (5.6) and solve for  $F_\eta$

$$F_\eta^2 = \chi_T^{\text{que}} \frac{2\pi}{g^2}. \quad (5.24)$$

Using the result in eq. (5.23) yields

$$F_\eta = 0.4243(76). \quad (5.25)$$

To check the lattice artifacts of this quantity, we compute  $F_\eta$  for more values of  $\beta$ .

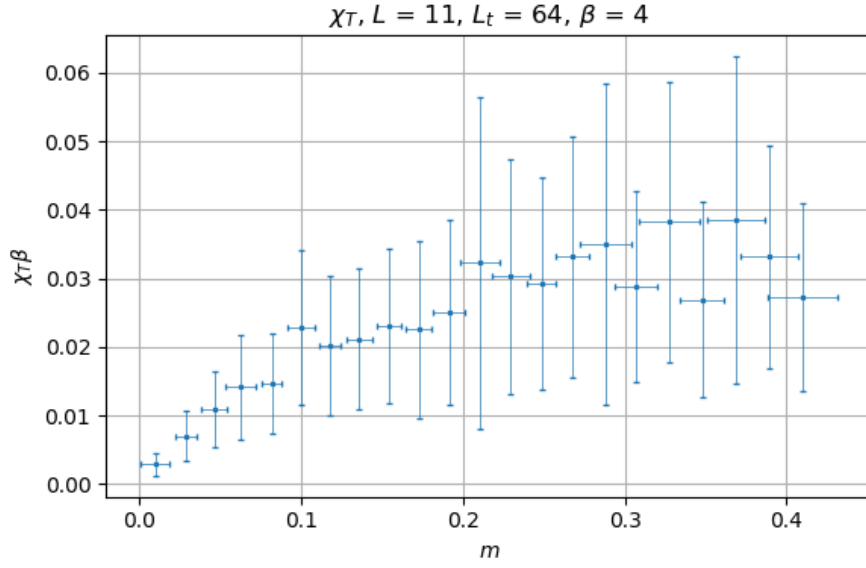
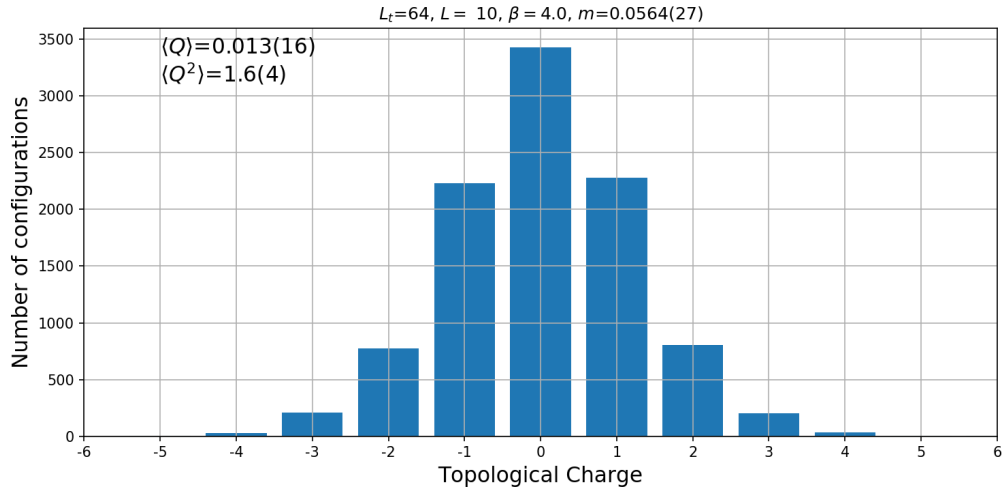
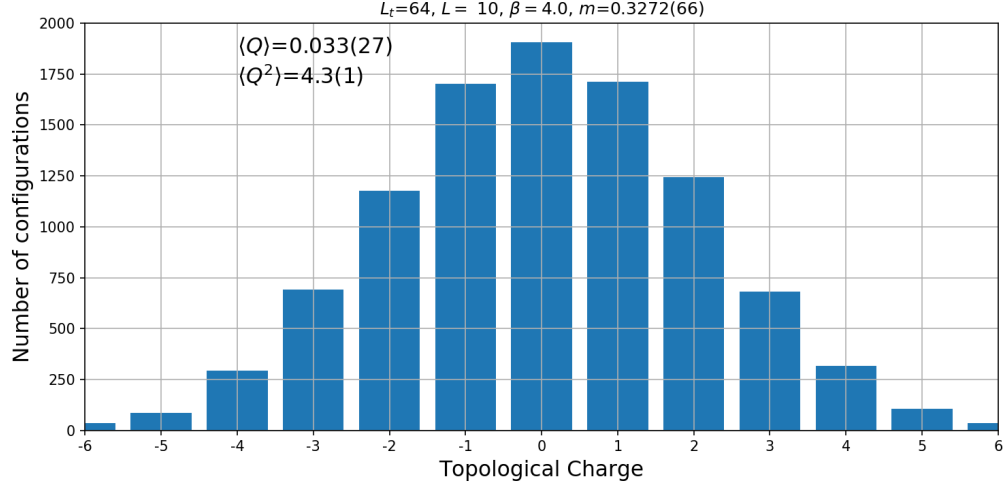


Figure 5.1: Topological susceptibility as a function of the fermion mass  $m$ , computed for  $10^3$  measurements with 10 sweeps between each of them on a  $11 \times 64$  lattice.  $\chi_T$  does not have a clear behavior for this number of measurements.

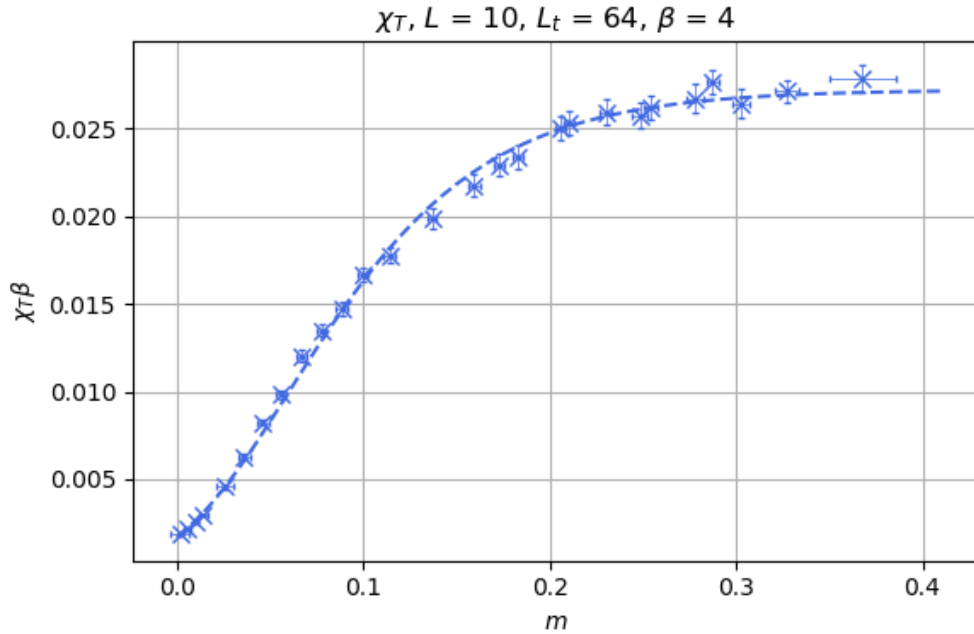


(a) Configurations sorted by their topological charge for  $m = 0.0564(27)$ .

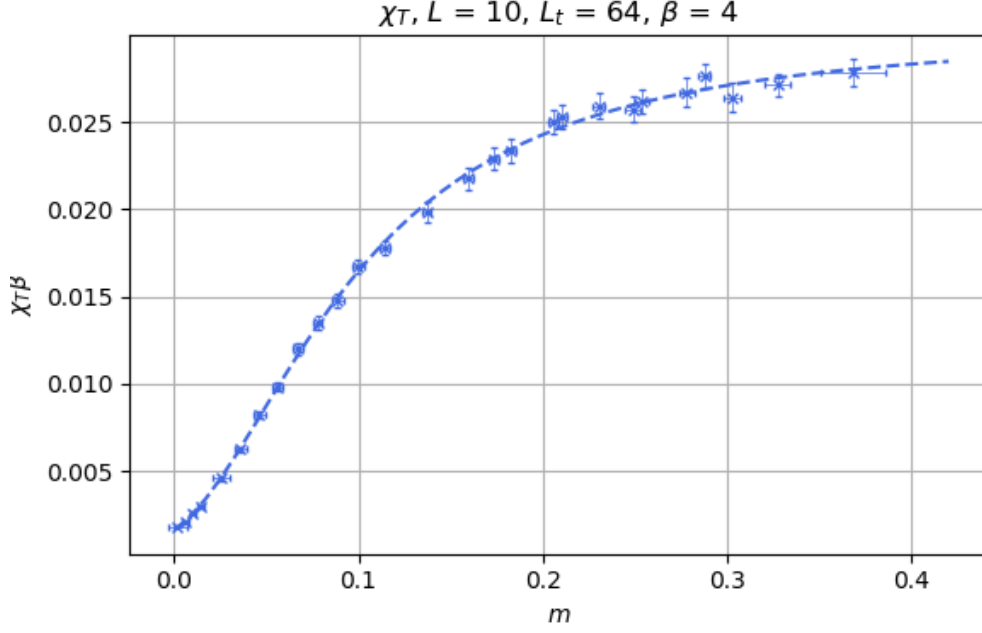


(b) Configurations sorted by their topological charge for  $m = 0.3272(66)$ .

Figure 5.2: Distribution of the Monte Carlo configurations in different topological sectors for  $\beta = 4$ . We see approximately a Gaussian distribution.  $m$  denotes the degenerate PCAC fermion mass. When the mass is smaller, the configurations occupy less topological sectors.



(a) A function of the form  $y = ae^{-be^{-cx}}$  was fitted to the data.



(b) We also fitted a function of the form  $y = \frac{a+bx+cx^2}{d+fx+gx^2}$ .

Figure 5.3: Topological susceptibility as a function of the degenerate fermion mass obtained with  $10^4$  measurements. The plots are in lattice unites. We performed two fits in order to extract the value of  $\chi_T$  when  $m \rightarrow \infty$ . The results yield  $\chi_T^{\text{que}}/g^2 = \chi_T^{\text{que}}\beta = 0.029(1)$ .

To do so, we performed more simulations to determine  $\chi_T$  in the quenched approximation by working with pure gauge theory, *i.e.* by generating Monte Carlo configurations using only the gauge action

$$S_G = \frac{1}{4} \int d^4x F_{\mu\nu} F_{\mu\nu}. \quad (5.26)$$

This is more convenient than extrapolating  $\chi_T$  to infinite  $m$ , because the simulations are faster and they yield results for  $m \rightarrow \infty$ . Still, the extrapolation of  $\chi_T$  to infinite  $m$  works as a cross-check with the results of  $\beta = 4$  that we obtain with the quenched simulations.

In figure 5.4, we show  $\chi_T^{\text{que}}\beta$  for different lattices of dimension  $L \times L$  and  $\beta = 2, 3, 4, 5, 6, 7$  and 8. We took  $10^4$  measurements separated by 10 sweeps for  $\beta = 2$  and 3;  $10^4$  measurements separated by 100 sweeps for  $\beta = 4$  and 5 and  $10^4$  measurements separated by  $10^3$  sweeps for  $\beta = 6, 7$  and 8. In table 5.1 we show  $\chi_T^{\text{que}}\beta$  for the different  $\beta$  values that we simulated, together with  $F_\eta$  computed with the Witten-Veneziano formula.

$\beta$	$\chi_T^{\text{que}}\beta$	$F_\eta$
2	0.0389(2)	0.495(1)
3	0.0335(3)	0.459(2)
4	0.0304(2)	0.437(1)
5	0.0285(4)	0.423(3)
6	0.0283(4)	0.422(2)
7	0.0261(11)	0.404(9)
8	0.0256(19)	0.399(15)

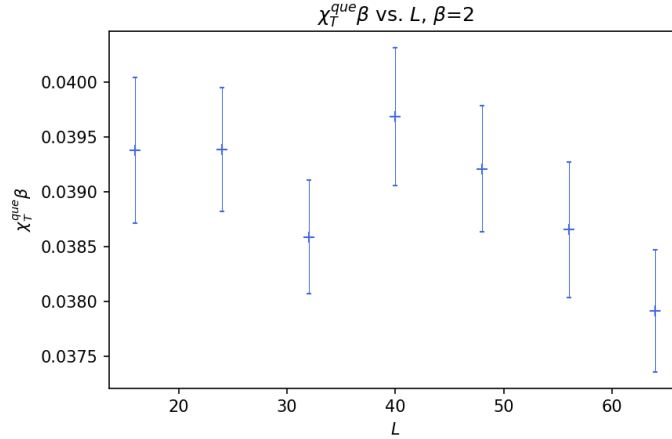
Table 5.1: Results of  $\chi_T^{\text{que}}\beta$  and  $F_\eta$  for different  $\beta$  values obtained with pure gauge theory simulations.

We observe that  $\chi_T^{\text{que}}\beta$  still depends on  $\beta$ . As  $\beta$  increases,  $\chi_T^{\text{que}}\beta$  decreases monotonically. For  $\beta = 4$  the number that we obtain by means of the quenched simulations is compatible, within errors, with the large  $m$  extrapolation that we performed before. In figure 5.5, we show a comparison of our results for  $\chi_T^{\text{que}}\beta$  with the values of refs. [5, 9]. Since  $\chi_T^{\text{que}}\beta$  is not independent of  $\beta$ ,  $F_\eta$  also has lattice artifacts. We can perform an extrapolation to the continuum limit by fitting the ansatz  $\chi_T^{\text{que}}\beta = a + b/\beta$ , where  $a$  and  $b$  are fit parameters, in order to determine  $F_\eta$ . The extrapolation yields

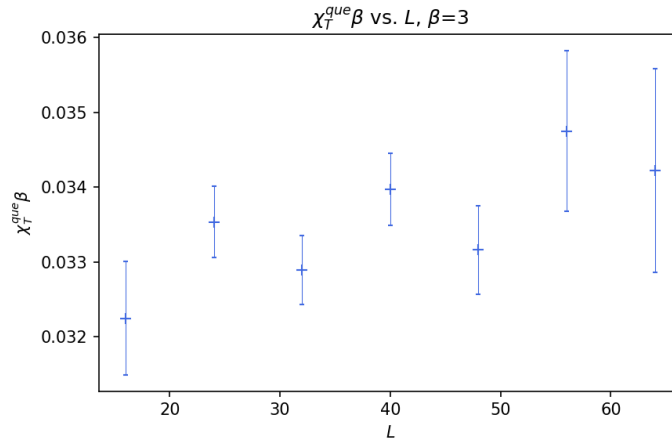
$$\chi_T^{\text{que}}\beta = 0.0223(3), \quad F_\eta = 0.374(3). \quad (5.27)$$

The result of eq. (5.27) is slightly below the theoretical prediction for infinite volume and in the continuum, given by eq. (5.17). We also compare our result of  $\chi_T^{\text{que}}\beta$  for large  $\beta$  with the value that was obtained in ref. [10]:  $\chi_T^{\text{que}}\beta \simeq 0.023$ . Our result is in agreement with this value.

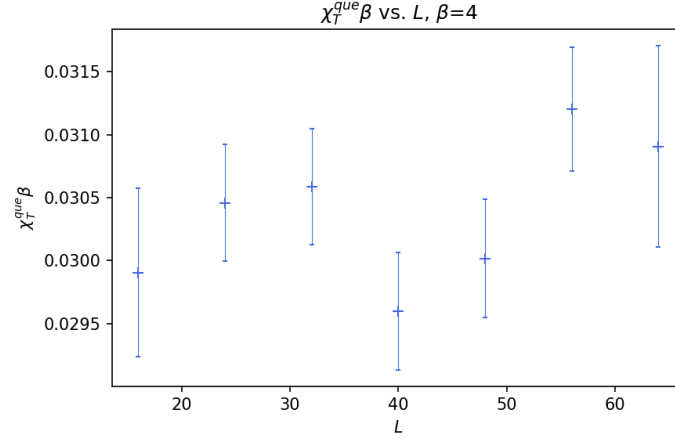
When we compare  $F_\eta$  with the value that we obtained in the  $\delta$ -regime:  $F_\pi = 0.6688(5)$ , we observe that they do not agree. Furthermore, in the  $\delta$ -regime the result is essentially independent of  $\beta$ , so the lattice artifacts are mild, in contrast to the outcome of  $F_\eta$ . This confirms that the hypothesis that  $F_\eta$  could be equal to  $F_\pi$  in the Schwinger model is not correct, although they are of the same order of magnitude.



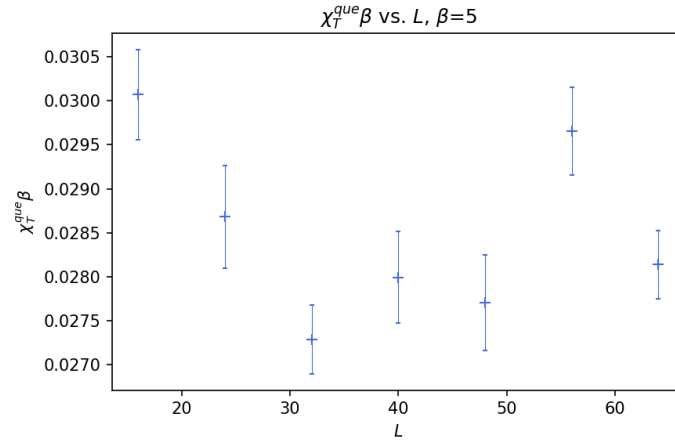
(a)  $\chi_T^{\text{que}}\beta$  vs.  $L$  for  $\beta = 2$ . An average yields  $\chi_T^{\text{que}} = 0.0389(2)$ .



(b)  $\chi_T^{\text{que}}\beta$  vs.  $L$  for  $\beta = 3$ . An average yields  $\chi_T^{\text{que}} = 0.0335(3)$ .



(c)  $\chi_T^{\text{que}} \beta$  vs.  $L$  for  $\beta = 4$ . An average yields  $\chi_T^{\text{que}} = 0.0304(2)$ .



(d)  $\chi_T^{\text{que}} \beta$  vs.  $L$  for  $\beta = 5$ . An average yields  $\chi_T^{\text{que}} = 0.0285(4)$ .

Figure 5.4:  $\chi_T \beta$  measured for different  $\beta$  and lattices of dimensions  $L \times L$ .

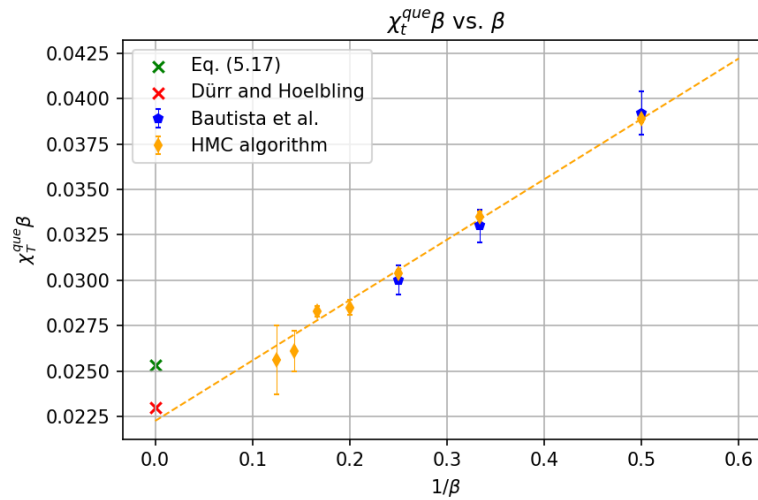


Figure 5.5:  $\chi_T^{\text{que}} \beta$  vs.  $1/\beta$ . Bautista *et al.* refers to ref. [9] and Dürr, Hoelbling to ref. [10]. HMC algorithm denotes the results that we computed with pure gauge theory simulations. In order to determine  $\chi_T^{\text{que}} \beta$  in the continuum we fitted a function of the form  $\chi_T^{\text{que}} \beta = a + b/\beta$ , which yielded  $\chi_T^{\text{que}} \beta = 0.0223(3)$ .



## *Bibliography*

---

- [1] E. Witten. Current Algebra Theorems for the U(1) Goldstone Boson. *Nucl. Phys. B*, 156:269–283, 1979.
- [2] G. Veneziano. U(1) Without Instantons. *Nucl. Phys. B*, 159:213–224, 1979.
- [3] P.A. Zyla et al. Review of Particle Physics. *Prog. Theor. Exp. Phys.*, 2020:083C01, 2020.
- [4] E. Seiler and I. O. Stamatescu. Some remarks on the Witten-Veneziano formula for the  $\eta'$  mass. *MPI-PAE-PTh-10-87*.
- [5] E. Seiler. Some more remarks on the Witten-Veneziano formula for the eta-prime mass. *Phys. Lett. B*, 525:355–359, 2002.
- [6] P. H. Damgaard, H. B. Nielsen, and R. Sollacher. Gauge symmetric approach to effective Lagrangians: The eta-prime meson from QCD. *Nucl. Phys. B*, 414:541–578, 1994.
- [7] C. R. Gattringer, I. Hip, and C. B. Lang. Quantum fluctuations versus topology: A Study in U(1)<sub>2</sub> lattice gauge theory. *Phys. Lett. B*, 409:371–376, 1997.
- [8] S. Dürr, Z. Fodor, C. Hoelbling, and T. Kurth. Precision study of the SU(3) topological susceptibility in the continuum. *JHEP*, 04:055, 2007.
- [9] I. Bautista, W. Bietenholz, A. Dromard, U. Gerber, L. Gonglach, C. P. Hofmann, H. Mejía, and M. Wagner. Measuring the Topological Susceptibility in a Fixed Sector. *Phys. Rev. D*, 92:114510, 2015.
- [10] S. Dürr and C. Hoelbling. Scaling tests with dynamical overlap and rooted staggered fermions. *Phys. Rev. D*, 71:054501, 2005.